

## Supplementary information

### **Ultrafine Ru nanoparticles as efficient HER electrocatalyst for large current density in alkaline media by electronic communication of Ru-O bonds**

Weihang Feng, Yongqiang Feng\*, Yingrui He, Junsheng Chen, Hai Wang, Tianmi Luo, Yuzhu Hu, Chengke Yuan, Liyun Cao, Liangliang Feng, Jianfeng Huang

School of Materials Science and Engineering, Shaanxi Key Laboratory of Green Preparation and Functionalization for Inorganic Materials, Shaanxi University of Science and Technology, Xi'an, 710021, People's Republic of China.

E-mail address: fengyq@sust.edu.cn.

## Materials

All reagents were used as received without any purification. Ruthenium trichloride ( $\text{RuCl}_3$ ), Pt/C (20 wt%), Nafion solution (5%) and potassium hydroxide ( $\text{KOH}$ ,  $\cong 95\%$ ) were purchased from Sigma-Aldrich. Fullerene ( $\text{C}_{60}$ ) was purchased from Xiamen Funano New Material Technology Co., Ltd.. Toluene ( $\text{C}_7\text{H}_8$ ,  $\cong 99.5\%$ ), isopropyl alcohol (IPA,  $(\text{CH}_3)_2\text{CHOH}$ ,  $\cong 99.7\%$ ), ethanol ( $\text{EtOH}$ ,  $\text{CH}_3\text{CH}_2\text{OH}$ , 99.7%), methanol ( $\text{MeOH}$ ,  $\text{CH}_3\text{OH}$ , 99%), tetrabutylammonium hydroxide (TBAH, 50% in water) and hydrogen peroxide ( $\text{H}_2\text{O}_2$ , 40%) were received from Sinopharm Chemical Reagent Co., Ltd.. Deionized water (DW, 18.25  $\text{M}\Omega/\text{cm}$ ) was obtained from the ultra-pure purification system (ULUPURE, UPDR-I-10T).

## Materials Characterization.

X-ray diffraction (XRD) patterns of the electrocatalysts were tested on a Rigaku D/max-2200PC diffractometer (Japan) using  $\text{Cu K}\alpha$  radiation ( $\lambda = 1.5406 \text{ \AA}$ ). High-resolution Transmission Electron Microscope (HRTEM) images and EDS mapping images were recorded using a JEOL JEM-2010 field-emission transmission electron microscope with an accelerating voltage of 200 kV. The chemical bonding states and compositions of the samples were processed by Fourier transform infrared spectroscopy (FT-IR) in the range of 4000 to 400  $\text{cm}^{-1}$  on a Bruker vector-80 installation. Raman spectra was collected on a Renishaw-invia Microscopic confocal laser Raman spectrometer with 532 nm as the excitation laser. The pyrolysis process of the precursors was characterized by thermogravimetry and differential thermal analysis (TG/DTA) using Universal V4.5A TA Instruments from room temperature to 800  $^\circ\text{C}$

in an N<sub>2</sub> atmosphere with a heating rate of 5 °C min<sup>-1</sup>. Deionized water (DW, 18.25 MΩ/cm) was obtained from the ultra-pure purification system (ULUPURE, UPDR-I-10T).

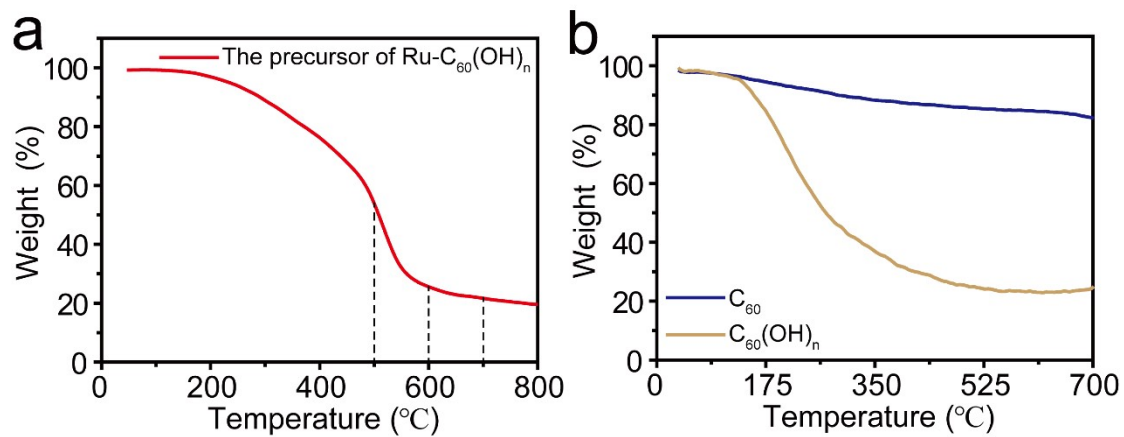


**Fig. S1.** Typical TG analysis of a) the precursor of Ru-C<sub>60</sub>(OH)<sub>n</sub>, and b) C<sub>60</sub> and C<sub>60</sub>(OH)<sub>n</sub>.

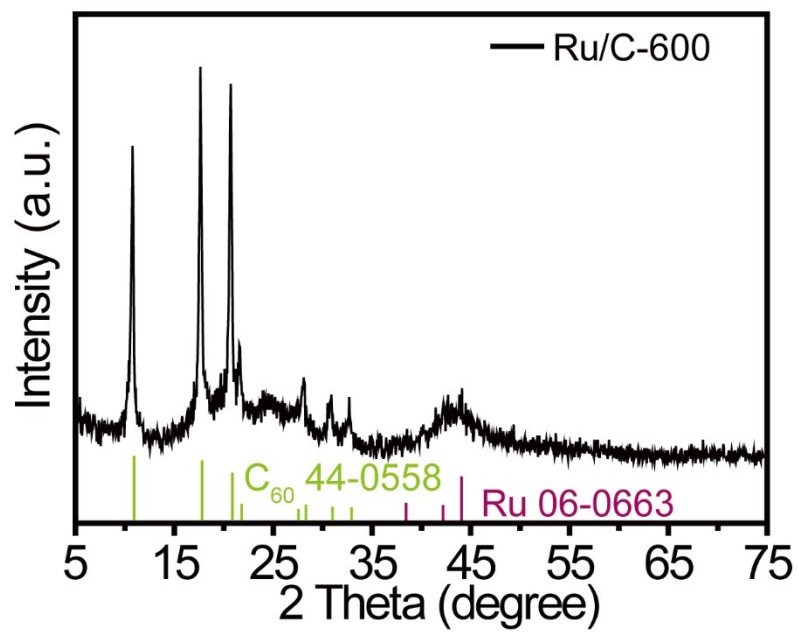


**Fig. S2.** The XRD pattern of Ru/C-600.

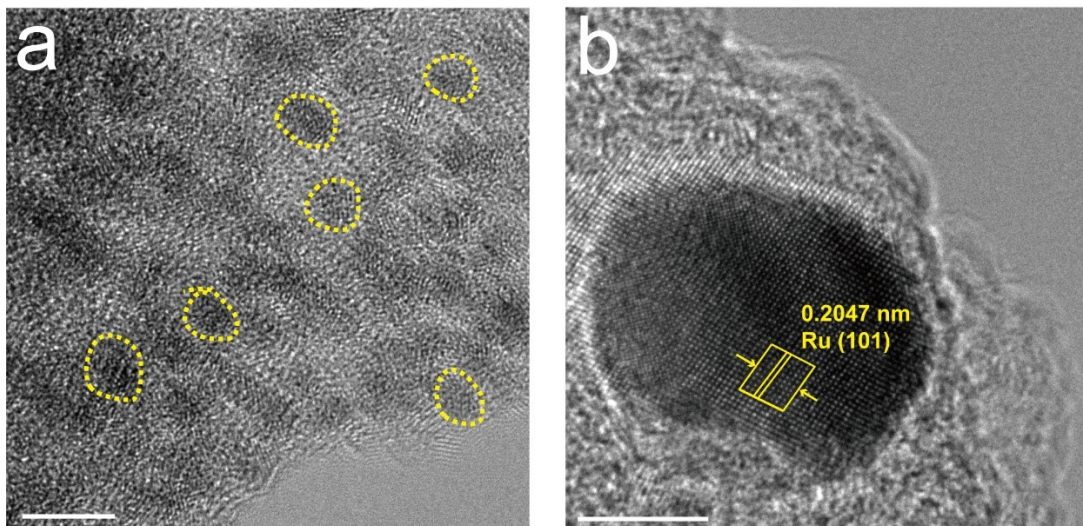


**Fig. S3.** HRTEM images of a) Ru-O/C-500 and b) Ru-O/C-700. Scale bar: 5 nm.

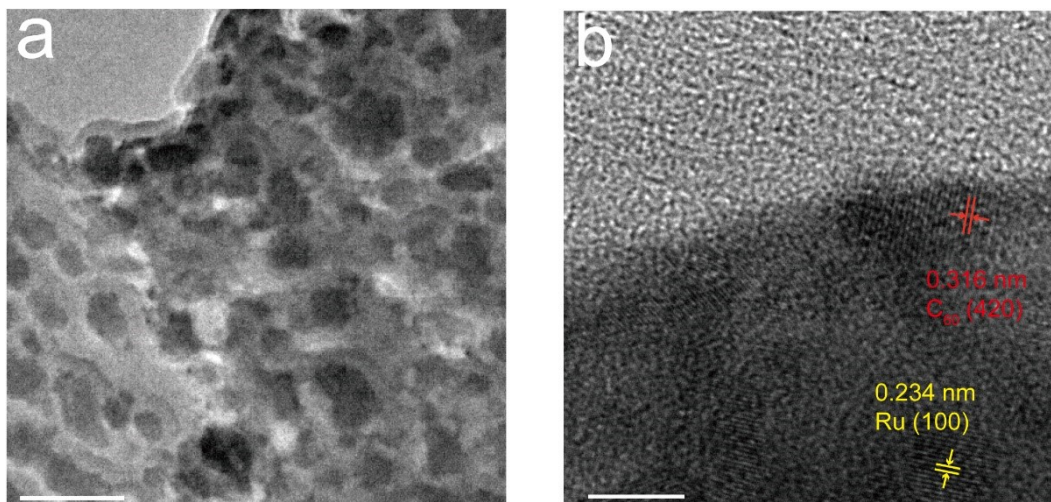


**Fig. S4.** TEM images of Ru/C-600. Scale bar a) and b): 100 nm and 5 nm.

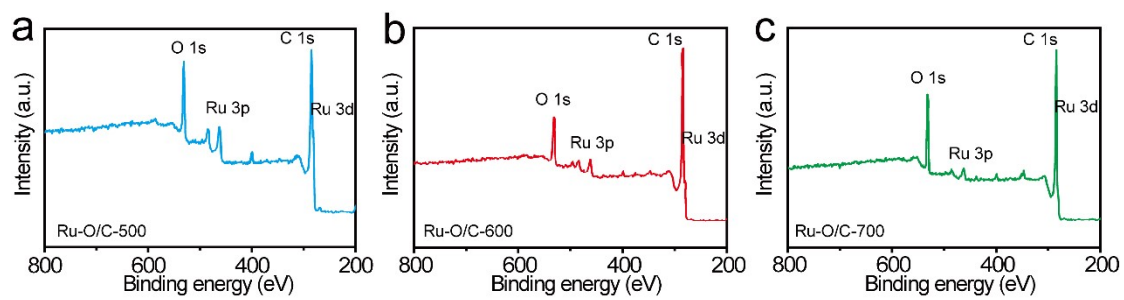


**Fig. S5.** X-ray photoelectron spectroscopy studies. XPS full survey spectra of (a) Ru-O/C-500, (b) Ru-O/C-600, and (c) Ru-O/C-700.



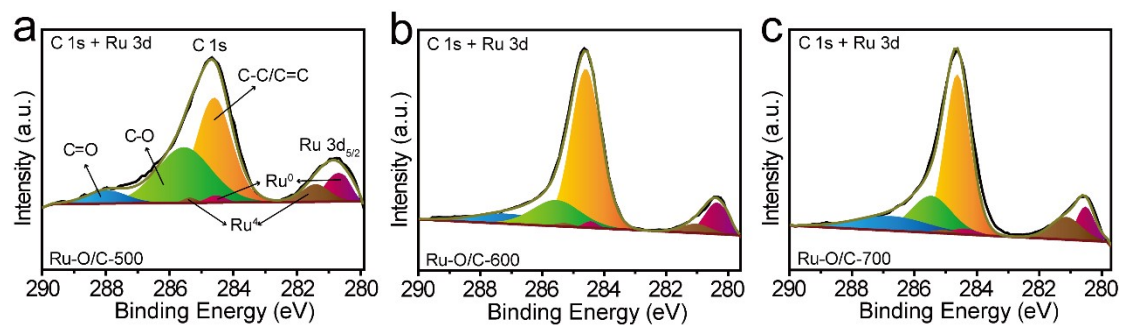


**Fig. S6.** High-resolution XPS spectra for C 1s and Ru 3d of (a) Ru-O/C-500, (b) Ru-O/C-600, and (c) Ru-O/C-700.

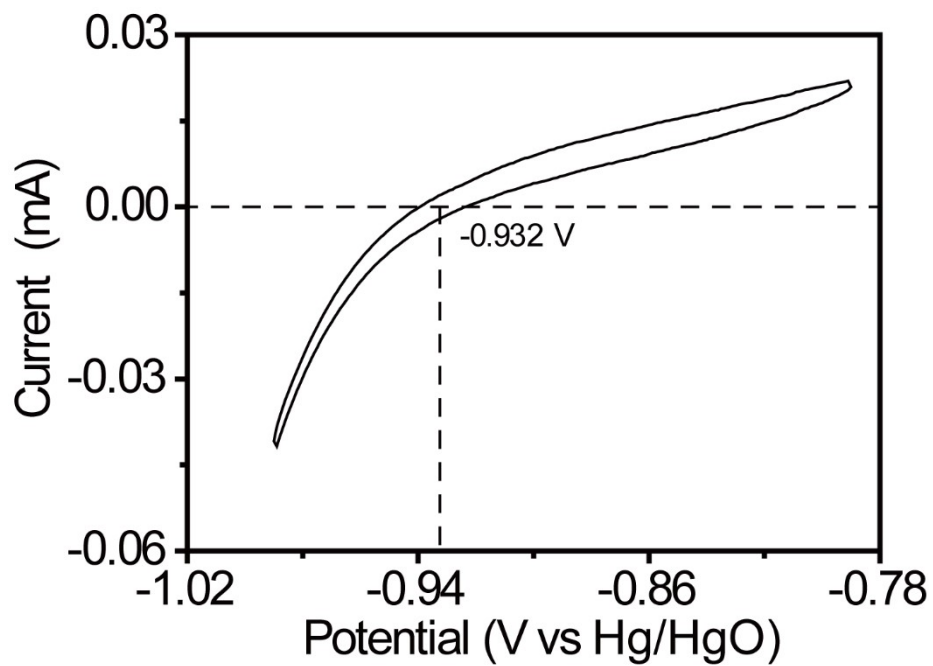


**Fig. S7.** Polarization curve of the Hg/HgO reference electrode calibrated against RHE in H<sub>2</sub>-saturated 1M KOH electrolyte<sup>1</sup>. Potential scan rate at 10 mV s<sup>-1</sup>

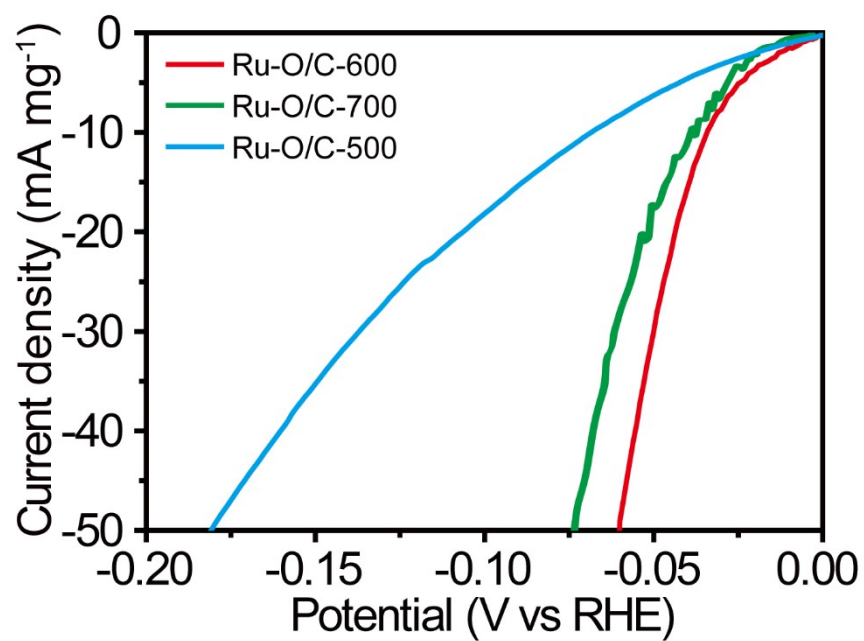


**Fig. S8.** LSV curves of the Ru-O/C-500, Ru-O/C-700, and Ru-O/C-600 normalized by Ru content in each sample.

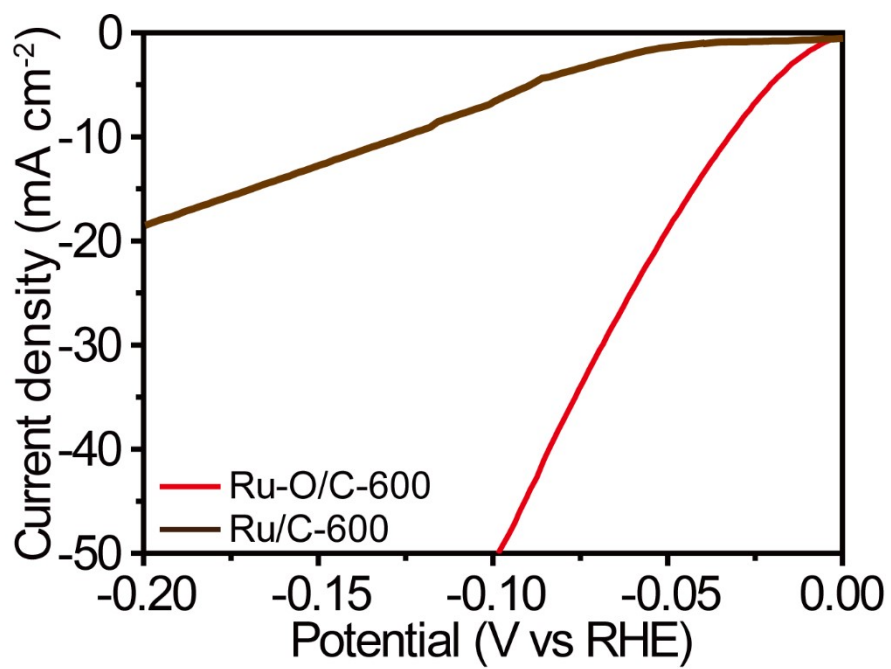


**Fig. S9.** LSV curves of the Ru/C-600 and Ru-O/C-600.

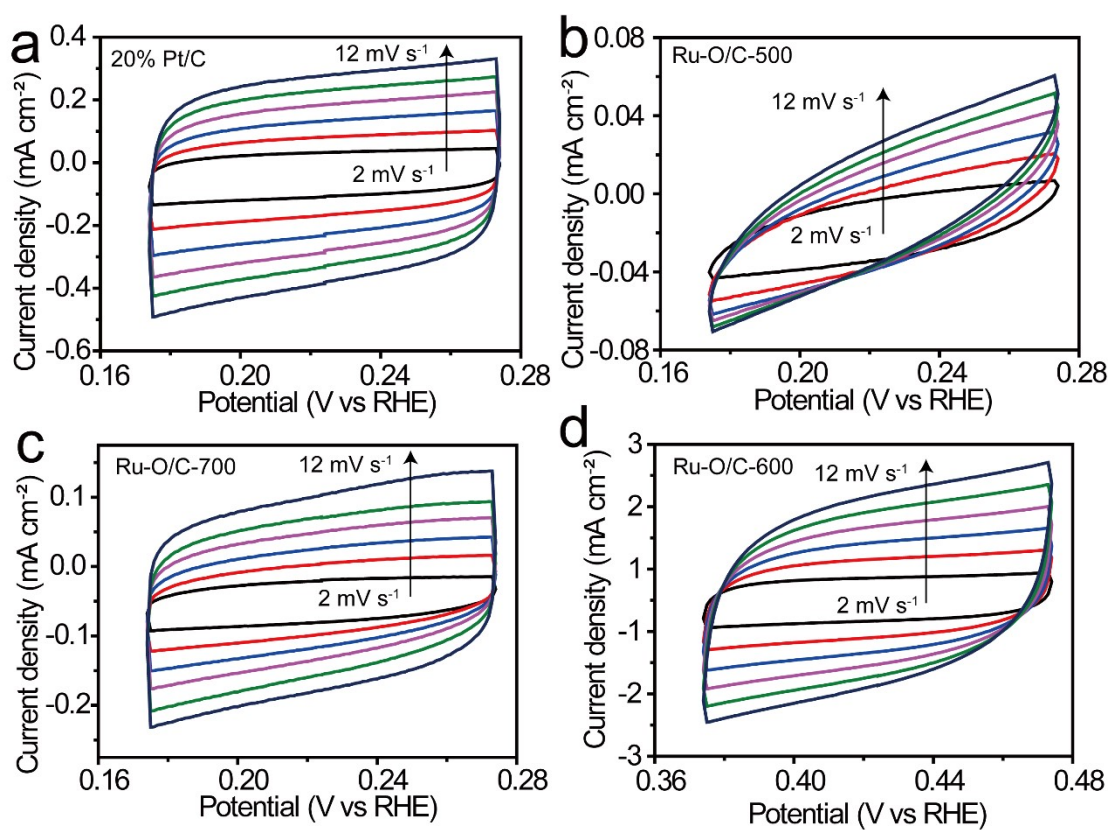


**Fig. S10.** a), b), c) and d) HER CV curves of the 20% Pt/C, Ru-O/C-500, Ru-O/C-700, and Ru-O/C-600 obtained at different scan rates between 2  $\text{mV}$  and 12  $\text{mV}$  in 1 M  $\text{KOH}^{2,3}$ , respectively.

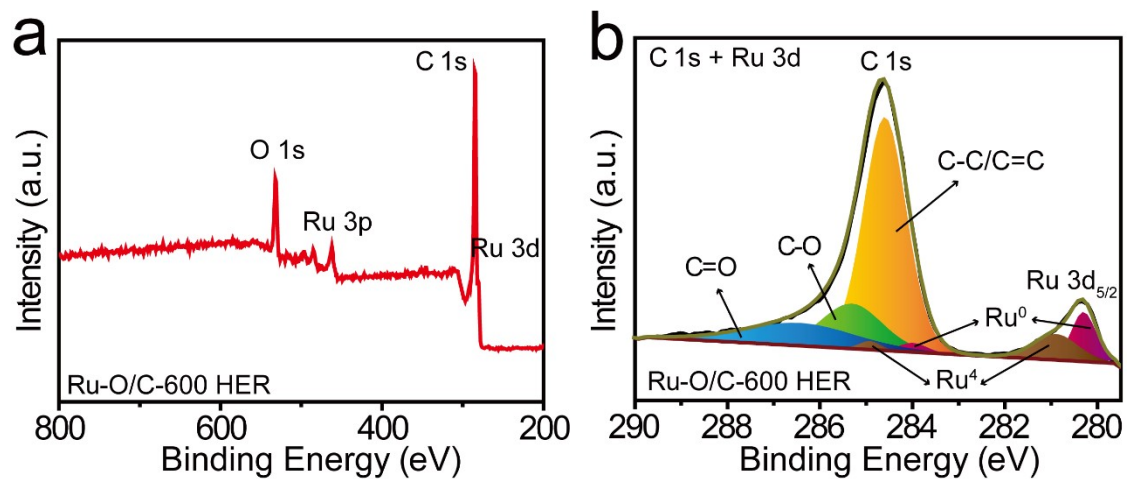


**Fig. S11.** (a) XPS survey spectra of Ru-O/C-600 after long-time stability test. (b) High-resolution XPS spectra for C 1s and Ru 3d of Ru-O/C-600 after long-time stability test.

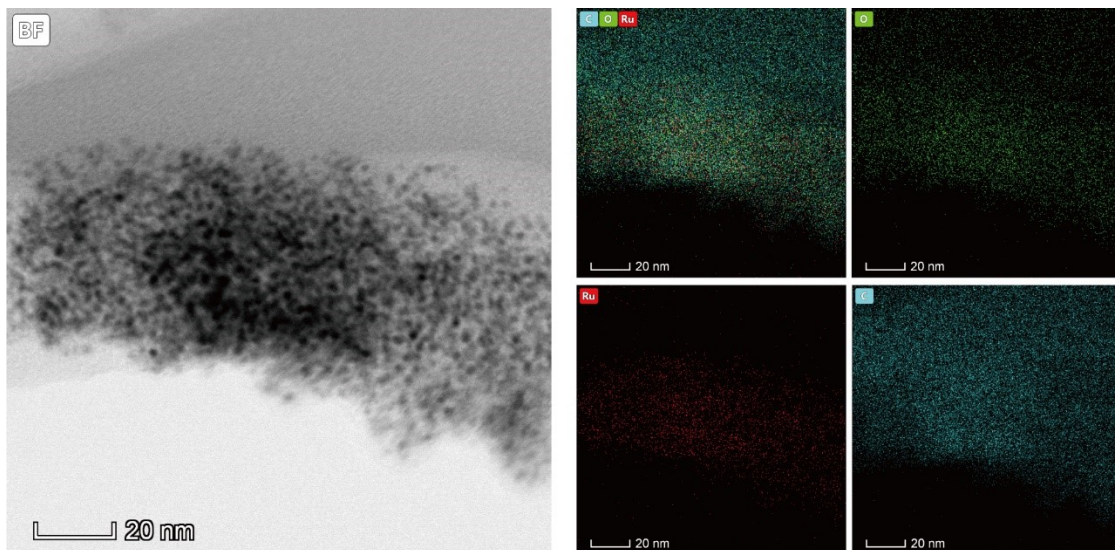


**Fig. S12.** TEM and element mapping images of Ru-O/C-600 after HER. Scale bar: 20 nm.

**Table S1.** a)  $I_D/I_G$  ratio of Raman spectra among Ru-O/C-600, Ru-O/C-700 and Ru-O/C-500.

<b>Sample</b>	<b><math>I_D/I_G</math></b>
<b>Ru-O/C-600</b>	0.82
<b>Ru-O/C-700</b>	0.78
<b>Ru-O/C-500</b>	0.98



**Table S2.** Comparison of HER activity data for test catalysts in this experiment.

<b>Sample</b>	<b><math>\eta_{10}</math> (mV)</b>	<b>Tafel plots (mV dec<sup>-1</sup>)</b>	<b>R<sub>ct</sub> (<math>\Omega</math>)</b>	<b>C<sub>dl</sub> (mF cm<sup>-2</sup>)</b>
<b>Ru-O/C-600</b>	32	51.8	12.8	117.5
<b>Ru-O/C-700</b>	75	99.8	40.5	10.8
<b>Ru-O/C-500</b>	190	236.9	81.5	1.5
<b>20% Pt/C</b>	46	61.2	29.8	26.1

**Table S3.** Summary of recently reported HER catalysts in 1 M KOH electrolyte.

No.	Catalyst	$\eta_{10}$ (mV)	reference
1	Pd@Ru NRs	30	ACS Appl. Mater. Interfaces 2018, 10, 34147-34152.
2	Ru/Co <sub>3</sub> O <sub>4</sub> NWs	30.98	Nano Energy 2021, 85, 105940.
3	Ru-Ni@Ni <sub>2</sub> P-HNRs	31	J. Am. Chem. Soc. 2018, 140, 2731-2734.
4	Ru-O/C-600	32	this work
5	NiRu@N-C (S-2)	32	J. Mater. Chem. A 2018, 6, 1376-1381.
6	Ru/Ni-MoS <sub>2</sub>	32	Appl. Catal. B 2021, 298, 120557.
7	Ru-MoO <sub>2</sub>	35	J. Mater. Chem. A 2017, 5, 5474.
8	Ru@NG-4	40	Sustain. Energy Fuels 2017, 1, 1028-1033.
9	Ru <sub>2</sub> Ni <sub>2</sub> SNs	40	Nano Energy 2018, 47, 1-7.
10	RuO <sub>2</sub> /N-C	40	ACS Sustainable Chem. Eng. 2018, 6, 11529-11535.
11	a-RuTe <sub>2</sub> PNRs	41	Nat. Commun. 2019, 10, 5692.
12	Pd <sub>3</sub> Ru/C	42	ACS Catal. 2019, 9, 9614.
13	Ru ND/C	43.4	Chem. Commun. 2018, 54, 4613-4616.
14	CoRu@NC	45	Nanotechnology 2018, 29, 225403.
15	STRO	46	Nat. Commun. 2020, 11, 5657.
16	RuNC700	47	Nat. Commun. 2019, 10, 631.
17	Ru@CoN-CNTs-2	48	ACS Sustainable Chem. Eng. 2020, 8, 24, 9136-9144.
18	Ru <sub>2</sub> P@PNC/CC-900	50	ACS Appl. Energy Mater. 2018, 1, 314-3150.
19	Ru <sub>1</sub> CoP/CDs-1000	51	Angew. Chem. Int. Ed. 2021, 60, 7234-7244.

<b>20</b>	Ni <sub>1.5</sub> Co <sub>1.4</sub> P@Ru	52	Chem. Commun. 2017, 53, 13153-13156.
<b>21</b>	RuP <sub>2</sub> @NPC	52	Angew. Chem. Int. Ed. 2017, 56, 11559-11564.
<b>22</b>	Ru/Co <sub>4</sub> N-CoF <sub>2</sub>	53	Chem. Eng. J. 2021, 414, 128865.
<b>23</b>	Ru/C- H <sub>2</sub> O/CH <sub>3</sub> CH <sub>2</sub> OH	53	Appl. Catal. B. 2019, 258, 117952.
<b>24</b>	Sr <sub>2</sub> RuO <sub>4</sub>	61	Nat. Commun. 2019, 10, 149.
<b>25</b>	ah-RuO <sub>2</sub> @C	63	Nano Energy 2019, 55, 49-58.
<b>26</b>	RuP <sub>x</sub> @NPC	74	ChemSusChem 2018, 11, 743-752.
<b>27</b>	SA-Ru-MoS <sub>2</sub>	76	Small Methods 2019, 1900653.
<b>28</b>	RuP <sub>2</sub> PC	79	J. Mater. Chem. A, 2021, 9, 12276-12282.
<b>29</b>	Cu <sub>2-x</sub> S@Ru NPs	82	Small 2017, 13, 1700052.
<b>30</b>	CoRu-OA@HNC-2	85	ACS Appl Mater Interfaces, 2020, 12, 51437-51447.
<b>31</b>	RuO <sub>2</sub> -NWs@g-CN	95	ACS Appl. Mater. Interfaces 2016, 8, 28678-28688.

## Reference

1. C. Wei, R. R. Rao, J. Peng, B. Huang, I. E. L. Stephens, M. Risch, Z. J. Xu and Y. Shao-Horn, Recommended practices and benchmark activity for hydrogen and oxygen electrocatalysis in water splitting and fuel cells, *Adv. Mater.*, 2019, **31**, e1806296.
2. J. Wang, F. Xu, H. Jin, Y. Chen and Y. Wang, Non-noble metal-based carbon composites in hydrogen evolution reaction: fundamentals to Applications, *Adv Mater*, 2017, **29**, 1605838.
3. D. Voiry, M. Chhowalla, Y. Gogotsi, N. A. Kotov, Y. Li, R. M. Penner, R. E. Schaak and P. S. Weiss, Best practices for reporting electrocatalytic performance of nanomaterials, *ACS Nano*, 2018, **12**, 9635-9638.